

## **Overlap between COPD genetic association results and transcriptional quantitative trait loci**

Aabida Saferali<sup>1</sup>, Wonji Kim<sup>1</sup>, Robert P. Chase<sup>1</sup>, NHLBI TransOmics in Precision Medicine (TOPMed), Chris Vollmers<sup>2</sup>, Edwin K. Silverman<sup>1,2</sup>, Michael H. Cho<sup>1,3</sup>, Peter J. Castaldi<sup>1,4</sup>, Craig P. Hersh<sup>1,3\*</sup>

<sup>1</sup>Channing Division of Network Medicine, Brigham and Women's Hospital

<sup>2</sup>Department of Biomolecular Engineering, Cellular, Cellular, and Developmental Biology, University of California Santa Cruz

<sup>3</sup>Division of Pulmonary and Critical Care Medicine, Brigham and Women's Hospital

<sup>4</sup>Division of General Medicine and Primary Care, Brigham and Women's Hospital

\*Corresponding author

Email: [craig.hersh@channing.harvard.edu](mailto:craig.hersh@channing.harvard.edu)

Author contributions

Word count: 3274

## **Abstract**

### **Rationale:**

Genome-wide association studies (GWAS) have identified multiple genetic loci associated with chronic obstructive pulmonary disease (COPD). When integrated with GWAS results, expression quantitative trait locus (eQTL) studies can provide insight into biological mechanisms involved in disease by identifying single nucleotide polymorphisms (SNPs) that contribute to whole gene expression. However, there are multiple genetically driven regulatory and isoform-specific effects which cannot be detected in traditional eQTL analyses. Here, we identify SNPs that are associated with alternative splicing (sQTL) in addition to eQTLs to identify novel functions for COPD associated genetic variants.

### **Methods:**

We performed RNA sequencing on whole blood from 3743 subjects in the COPDGene Study. RNA sequencing data from lung tissue of 1241 subjects from the Lung Tissue Research Consortium (LTRC), and whole genome sequencing data on all subjects. Associations between all SNPs within 1000 kb of a gene (cis-) and splice and gene expression quantifications were tested using tensorQTL. In COPDGene a total of 11,869,333 SNPs were tested for association with 58,318 splice clusters, and 8,792,206 SNPs were tested for association with 70,094 splice clusters in LTRC. We assessed colocalization with COPD-associated SNPs from a published GWAS[1].

### **Results**

After adjustment for multiple statistical testing, we identified 28,110 splice-sites corresponding to 3,889 unique genes that were significantly associated with genotype in COPDGene whole blood, and 58,258 splice-sites corresponding to 10,307 unique genes associated with genotype in

LTRC lung tissue. We found 7,576 sQTL splice-sites corresponding to 2,110 sQTL genes were shared between whole blood and lung, while 20,534 sQTL splice-sites in 3,518 genes were unique to blood and 50,682 splice-sites in 9,677 genes were unique to lung. To determine what proportion of COPD-associated SNPs were associated with transcriptional splicing, we performed colocalization analysis between COPD GWAS and sQTL data, and found that 38 genomic windows, corresponding to 38 COPD GWAS loci had evidence of colocalization between QTLs and COPD. The top five colocalizations between COPD and lung sQTLs include *NPNT*, *FBXO38*, *HHIP*, *NTN4* and *BTC*.

### **Conclusions**

A total of 38 COPD GWAS loci contain evidence of sQTLs, suggesting that analysis of sQTLs in whole blood and lung tissue can provide novel insights into disease mechanisms.

## **Introduction**

Chronic obstructive pulmonary disease (COPD) is a complex disease characterized by irreversible airflow obstruction on lung function testing. The leading environmental risk factor for COPD is cigarette smoking, however, genetic factors have also been shown to play a role in disease susceptibility[2-5]. Genome-wide association studies (GWAS) have been used to identify genetic variants associated with COPD and lung function[1, 6-8]. However, as for most complex trait GWAS associations, the causal mechanisms are currently unknown. While it has been found that expression quantitative trait loci (eQTL) are enriched among GWAS loci, a large proportion of disease heritability remains unexplained by eQTLs [9]. Previous work has shown that splicing quantitative trait loci (sQTLs), in which genetic variants affect alternative splicing, can account for at least as many GWAS loci as eQTLs[10].

A recent genome wide association study for COPD including 35,735 cases and 222,076 controls from the UK Biobank and the International COPD Genetics Consortium identified 82 loci associated with COPD with genome wide significance[1]. Using S-PrediXcan[11], the authors discovered that 49 GWAS loci had evidence for genetically regulated expression associated with COPD using data from the Lung-eQTL consortium[1]. As S-PrediXcan is also influenced by linkage disequilibrium, most of the COPD GWAS loci are likely not explained using existing eQTLs.

Genomic loci identified as being eQTLs may also be sQTLs, as splicing is a common mechanism to alter total gene expression levels. In our previous work, we generated sQTLs in 376 subjects from the COPDGene study and found that these data could explain seven COPD GWAS associations, including the identification of *FBXO38* as a novel COPD susceptibility gene at 5q32 [10]. Here, we expand upon our findings by developing a large database of eQTLs

and sQTLs in RNA from lung tissue from 1,241 subjects and in RNA from blood from 3,743 subjects followed by colocalization analysis with COPD GWAS results.

## **Materials and Methods:**

### **Study Population**

This study included 3,713 non-Hispanic white and African American subjects from the COPDGene study and 1,241 subjects from the Lung Tissue Research Consortium (LTRC) (Table 1). COPDGene enrolled individuals between the ages of 45 and 80 years with a minimum of 10 pack-years of lifetime smoking history from 21 centers across the United States [12]. These subjects returned for a second study visit 5 years after the initial visit at which time they completed additional questionnaires, pre-and post-bronchodilator spirometry, chest computed tomography of the chest, and provided blood for complete blood counts (CBCs) and RNA sequencing. Samples were collected as part of the LTRC from individuals who were undergoing clinically indicated thoracic surgery procedures using a standardized protocol described in the original study design, which included pulmonary function testing, questionnaires, and chest CT [13].

### **RNA sequencing, alignment and count generation**

The protocols for RNASeq data generation and processing for COPDGene and LTRC have been previously described [14] [13]. Briefly, for LTRC, mRNA sequencing (RNAseq) was performed through the NHLBI TOPMed program at the University of Washington. Poly-A selection and cDNA synthesis was performed using the TruSeq Stranded mRNA kit (Illumina), and sequencing was performed on the NovaSeq6000 instrument. Sequences were aligned to GRCh38 using STAR (v2.6.1d) with the GENCODE release 29 reference. Gene-level expression quantification was performed using RSEM (v1.3.1). For COPDGene, globin reduction, ribosomal RNA depletion, and cDNA library prep was performed on total RNA from whole blood using the TruSeq Stranded Total RNA with Ribo-Zero Globin kit (Illumina, Inc.,

San Diego, CA), and sequencing was performed on Illumina platforms. Sequences were aligned to GRCh38 using STAR 2 pass alignment (v.2.5.2b). Gene-level expression quantification was performed using Salmon (v1.3.0) for pseudoalignment to GENCODE release 37 transcriptome, followed by summarization of isoform-level counts to gene-level counts using tximport (v.1.8.5) [15, 16]. Quantification of splicing ratios was performed in COPDGene and LTRC using Leafcutter with default parameters [17]. Intron ratios were calculated by determining how many reads support a given exon-intron junction in relation to the number of reads in that region.

### **Whole Genome Sequencing**

All samples were sequenced through the TOPMed program. This analysis uses Freeze 8 data.

### **eQTL and sQTL Analysis**

Gene expression counts were filtered to include only genes with at least 1 count per million in at least 20% of subjects, and the remaining counts were TMM normalized [18]. Leafcutter ratios were filtered to remove introns detected in less than 40% of individuals and introns with a standard deviation of less than 0.005 across subjects, and the remaining ratios were scale normalized (ie mean centered and divided by the standard error). TensorQTL [19] was used to test for association between genotypes of all SNPs within 1000 kb of the gene boundary (cis-) and quantifications of splicing or gene expression using linear models, adjusting for gender, batch, principal components of splicing or gene expression data and principal components of genetic ancestry. Calculation of principal components of genetic ancestry has been previously described [20]. A total of 8,792,206 variants (biallelic SNPs with MAF > 0.01) were tested for association with 58,258 splice sites (corresponding to 10,615 unique genes) and expression of 16,264 genes. Results were annotated using ANNOVAR [21] with annotations derived from dbSNP build 150.

## **Colocalization analysis**

Published GWAS data for COPD case-control status [1] were used for this analysis. Testing windows were generated by identifying all GWAS variants with  $p < 1 \times 10^{-5}$  and calculating non-overlapping windows of 1MB on either side of each SNP. Only windows containing sQTLs or eQTLs with  $FDR < 0.05$  were tested. For each window, Bayesian colocalization tests were performed using the Moloc R package [22] to quantify the probability that the GWAS and sQTL or eQTL associations were due to a shared causal variant. Windows with a colocalization posterior probability (CPP) of greater than 0.8 were reported. Fine mapping was performed on QTL results from selected regions of interest using SuSieR version 12.35, with in sample LD [23].

## **Long read RNA-seq analysis in human lung samples from the LTRC**

We conducted targeted Oxford Nanopore Technologies (ONT) long read sequencing on RNA from 170 human lung samples from the LTRC on genes selected from colocalization analysis. The enrichment and library generation procedures are described in detail in the Supplemental Methods. The final library was loaded onto a PromethION R10.4 flow cell and run at 400bp/s. Approximately once per day, flow cells were flushed and treated with DNase I, then loaded with additional library to increase sequencing throughput. Resulting raw reads were basecalled using the SUP model of guppy (v6) and consensus called and demultiplexed using C3POa (v2.3). R2C2 reads were analyzed to identify and quantify isoforms using version 3.5 of Mandalorian (<https://github.com/rvolden/Mandalorian-Episode-III>). Mandalorian was run twice to identify high abundance isoforms (>10% of total isoform expression; `-O 0,40,0,40 -r 0.1 -i 1 -w 1 -n 2 -R 5`) and high and low abundance isoforms (`-O 0,40,0,40 -r 0.01 -i 1 -w 1 -n 2 -R 5`).



## **Results:**

### Quantification of gene expression and RNA splicing in COPDGene blood and LTRC lung

Using RNASeq data from LTRC lung tissue (n=1241) and COPDGene whole blood (n=3713) we identified splice sites using Leafcutter [24], which identifies and quantifies intron exclusion. After filtering out splice sites with low usage, we identified a total of 223,128 splice sites, corresponding to 15,121 genes in LTRC, and 160,658 splice sites corresponding to 12,096 genes in COPDGene (Table 2). In both LTRC and COPDGene, the majority (50.1% and 51.0%, respectively) of identified splice sites were annotated in GENCODE, followed by cryptic 3', cryptic 5', cryptic unanchored splice sites (meaning both splice donor and acceptor were unannotated) and novel annotated pairs (Table 3). Gene expression of 16,266 genes in LTRC and 15,507 genes in COPDGene met expression thresholds (Table 2).

### Identification of eQTL and sQTLs in human lung tissue and whole blood

We next tested for association between genotype and gene expression or splicing to identify eQTLs and sQTLs in lung and blood. In LTRC lung tissue we identified 58,258 splice sites (corresponding to 10,615 genes) associated with at least one SNP with q-value<0.05; in COPDGene blood 60,291 splice sites (corresponding to 8,671 genes) were associated with at least one SNP (Table 2). In addition, we identified 12,225 genes associated with at least one SNP (eQTLs) in LTRC, and 15,279 eQTL genes in COPDGene. We found that 14,064 sQTL splice-site-SNP pairs (13%) were found in both blood and lung, while 6,353 eQTL gene-SNP pairs were shared between both tissues (25%) (Figure 1). In addition, we found that 5,787 sQTL gene-SNP pairs overlapped with eQTL gene-SNP pairs in LTRC (47%), while 7,455 sQTL gene-SNP pairs overlapped with eQTL gene-SNP pairs in COPDGene (49%).

### Functional annotation of sQTLs and eQTLs

Next we categorized eQTLs and sQTLs-SNPs on the basis of their location relative to the gene with which they were associated (Table 4). The genomic distribution of eQTLs and sQTLs was similar, with the largest proportion of variants located upstream of the gene region in both COPDGene (32.1% and 34.7 %, respectively) and LTRC (31.8% and 29.4%, respectively). The next most frequent SNPs were intronic, downstream of gene, intergenic, and 3' UTR variants. Only a small percentage of lead sQTL-SNPs directly modified a splice site. There was no difference in variant position in either eQTL vs sQTL and in COPDGene blood vs LTRC lung.

### Colocalization of QTLs with COPD Case-Control GWAS data

We next sought to identify eQTLs and sQTLs which contribute to COPD risk by performing genetic colocalization between the QTL data and COPD case-control GWAS data. Based on GWAS data, 239 genomic windows with COPD GWAS p-values  $< 5 \times 10^{-5}$  were identified, and of these, 237 contained sQTLs or eQTLs with q-value  $< 0.05$ . We also included colocalization results for 3' UTR alternative polyadenylation QTLs (apaQTLs) from our previous study [25]. We identified 38 windows with a colocalization posterior probability of association (PPA)  $> 0.8$  with either eQTL, sQTL or apaQTL data and GWAS p-value  $< 5.0 \times 10^{-8}$  (Table 5). We found that for 19 loci the strongest colocalization (largest PPA) with GWAS data was in LTRC, and for 19 loci the strongest colocalization was in COPDGene. In LTRC, the largest number of GWAS loci colocalized with sQTLs (9 loci), followed by eQTLs (7 loci) then apaQTLs (3 loci). In COPDGene, the majority of colocalizations were with sQTLs (15 loci), with only one locus colocalizing most strongly with eQTLs, and 3 with apaQTLs. We compared the colocalization findings with the target genes identified from the original GWAS analysis to determine whether the QTLs identified novel targets from previous analyses. We found that for 7 loci all genes

identified in the current QTL analysis were previously identified, and for 26 loci one or more new targets were found (Supplementary Table 1). For further characterization we focused on sQTL colocalizations in LTRC lung, with the top five colocalizations (by highest PPA) being *Nephronectin (NPNT)*, *F-box protein 38 (FBXO38)*, *Hedgehog interacting protein (HHIP)*, *Netrin 4 (NTN4)* and *Betacellulin (BTC)*. We have previously published on NPNT colocalizations in the lung [26], and for HHIP significant evidence suggests that the mechanism underlying the association is an eQTL effect [27]. *NTN4* appears to be a promoter usage eQTL instead of an sQTL. Therefore, we highlight the results for *FBXO38* and *BTC* below. All colocalization results are available online at (<https://copd-moloc.bwh.harvard.edu/>).

#### Characterization of sQTL for *FBXO38*

We first sought to replicate the association we previously characterized in 365 subjects from COPDGene between the rs7730971 (5:148411297:C:G) variant and *FBXO38* splicing in whole blood which colocalized with COPD GWAS findings [10]. Here, we identified two splicing clusters (ie a group of splice junctions with shared start or stop positions [24]) in lung tissue in *FBXO38* which were associated with COPD-related variants. First, we confirmed our previous finding that rs7730971 was significantly associated with inclusion of a 158 bp cryptic exon located between exons 9 and 10 (Figure 2). While significant colocalization was not detected using moloc, we previously found colocalization in this locus using eCaviar [28]. The G allele, which is associated with increased risk of COPD, is also associated with increased inclusion of the cryptic exon (Figure 2b). SpliceAI [29] indicates that rs7730971-G is predicted to slightly increase the splice acceptor strength of a splice site 217 bp upstream of the variant, which corresponds to the 5' splice acceptor of the cryptic exon, confirming that this is the likely causal variant. Using long-read sequencing we identified one isoform meeting expression thresholds

which includes the 158 bp cryptic exon (Figure 2c). This transcript includes a premature stop codon in the cryptic exon, and because this stop is more than 50 bases from the transcriptional stop, it would likely be subject to nonsense mediated decay [30]. This isoform is more abundant in the GG genotype compared to AA (5 reads vs 1). Supporting the finding that the transcript containing the cryptic exon is subject to nonsense mediated decay, we found that rs7730971 is also an eQTL for *FBXO38*, with the G allele associated with decreased expression (Figure 2d). We additionally identified a new colocalization between genetic variants in the *FBXO38/HTR4* region and inclusion of an exon at chr5: 148415241-148415387 (Supplementary Data).

#### Colocalization analysis of a genetic signal at *BTC*

Another significant colocalization between sQTLs and COPD GWAS findings was identified in LTRC lung tissue at the *BTC* locus where we found evidence of a shared genetic signal between variants associated with alternative inclusion of exon 4 of *BTC*, and COPD risk GWAS data (PPA=0.95) (Figure 3a). The lead colocalized variant was rs62316278 (4:74748514:C:T), and the COPD risk allele (C) is associated with increased inclusion of exon 4 (Figure 3b). This variant is within the 95% credible set for sQTL data using SuSie fine mapping, along with 42 additional variants. Of the variants in the 95% credible set, we found using SpliceAI that rs11938093-T (4:74750631:A:T) is associated with the gain of a splice donor 58 bp upstream of the SNP, corresponding to the splice donor of exon 4, as well as the gain of a splice acceptor 88 bp downstream of the SNP, corresponding to the splice acceptor of exon 4. Long read sequencing identified four high abundance isoforms for *BTC* (representing at least 10% of *BTC* expression each) (Figure 3c), and the proportion of isoforms containing exon 4 was higher in CC vs TT subjects (84% vs 48%, p=0.0003). These isoforms correspond to NM\_001729 (*BTC*-201, ENST00000395743.8) and NM\_001316963 (not included in ENSEMBL). NM\_001729

(including exon 4) is the primary version of *BTC*, and codes for a 178 amino acid protein, while NM\_001316963 codes for 129 amino acids.

## **Discussion:**

In this study we build upon our previous work characterizing COPD associated sQTLs in blood RNASeq data from COPDGene by generating a large dataset of eQTLs and sQTLs in human blood and lung tissue and identifying gene expression and splicing events, and we identify a substantial number of QTLs that suggest a functional mechanism for COPD GWAS loci. We found that approximately 50% of splice sites identified were not currently annotated, indicating the vast amount of currently uncharacterized splicing variability present in the transcriptome. Among the 223,128 splice sites identified in LTRC lung tissue and 160,658 in COPDGene blood, we found that 58,258 (26%) and 60,291 (38%) splice sites, respectively, were associated with at least one variant within 1 MB (FDR<5%). In addition, of the 16,266 genes expressed in LTRC and 15,507 genes expressed in COPDGene, 12,225 (75%) and 15,279 (99%) of genes, respectively, were associated with at least one SNP. The majority of eQTL and sQTL SNPs were located upstream of the gene body or in intronic regions, suggesting that many sQTLs function through long range or indirect effects, as opposed to modifying splice donors or acceptors directly. We identified 38 loci (corresponding to 33 of the original 82 GWAS loci) with significant colocalization with either eQTL, sQTL or apaQTL data, and of these, 9 loci colocalized most strongly with LTRC sQTLs, and 15 with COPDGene sQTLs. We confirmed our previous sQTL findings in the *FBXO38/HTR4* region, and identified *BTC* as additional novel target with strong COPD colocalization.

Here, we validated in lung tissue our previous findings from blood that rs7730971 is associated with splicing of a cryptic exon in *FBXO38*. Open reading frame analysis of the full

length transcript sequence indicates that the cryptic exon contains a premature stop codon, and therefore this transcript is likely subject to nonsense mediated decay. We also found that rs7730971 is associated with gene expression of *FBXO38*, with decreased expression with the G allele, which is also the variant associated with a bioinformatically predicted increase in nonsense mediated decay. Therefore, the likely mechanism underlying the eQTL association is degradation of *FBXO38* as result of increased inclusion of a cryptic exon which results in a transcript with an early stop codon. This is an example of a mechanism by which an eQTL can be mediated through an sQTL.

The allele associated with decreased expression of *FBXO38* is associated with increased COPD risk, suggesting that *FBXO38* plays a protective role against COPD. We found an additional colocalization between rs10037493, the most significant COPD GWAS SNP in the locus, and an additional *FBXO38* exon. The long read sequences containing this exon correspond to two predicted isoforms, each encoding shorter proteins than the most abundant isoform. The COPD risk allele is associated with the shortened isoforms, indicating that the full length *FBXO38* isoform is protective. These shortened isoforms lack the F-box domain, which is a component of all members of F-box proteins, including *FBXO38*. F-box proteins are a component of the ubiquitin ligase complex and also function as transcription factors [31]. *FBXO38* specifically is a coactivator of the Kruppel-like factor 7 (KLF7) zinc finger transcription factor [32, 33]. While little is known about the function of *FBXO38* and its potential role in COPD, the lack of the F-box protein, which is responsible for protein-protein interactions, in disease associated isoforms indicates that *FBXO38* interactions are critical for protection against COPD.

We identified an additional colocalization between the COPD GWAS and a novel candidate gene, *BTC*. We specifically found that rs62316278, the lead GWAS SNP in the *BTC* region, is also associated with splicing of exon 4, with the risk allele (C), increasing exon 4 inclusion. The primary form of *BTC*, NM\_001729, includes exon 4, and rs62316278-C is associated with an increased proportion of NM\_001729 relative to NM\_001316963, a protein coding isoform which lacks exon 4. This suggests that reduced inclusion of exon 4 is protective for COPD. *BTC* is a member of the epidermal growth factor (EGF) family of peptide ligands, and a ligand for epidermal growth factor receptor (EGFR). Human *BTC* encodes a 178-amino acid product corresponding to the *BTC* precursor protein (pro-*BTC*) and contains several domains including a signal peptide, an EGF motif and transmembrane domains [34]. The mature sequence of *BTC* is cleaved from the extracellular domain of *BTC* to produce an 80 amino acid protein. Based on the structure of other members of the EGF family, exon 4 is predicted to make up the third loop of the EGF-like motif and the transmembrane domain [34]. The EGF domain is critical to binding with EGF ligands, and therefore the isoform lacking exon 4 could be predicted to have impaired function. Several previous studies have linked *BTC* expression to COPD, and *BTC* has been found to be higher in ex-smokers with COPD than without COPD, has been associated with emphysema in alpha-1 antitrypsin deficiency [35] and has been found elevated in acute exacerbations in COPD [36]. More targeted work is needed to investigate the function of *BTC* isoforms in COPD.

The major strength of this study is the large sample size which allowed us to comprehensively characterize alternative splicing in whole blood and lung tissue. Our sample size significantly exceeds that of other commonly used resources such as The Genotype Tissue Expression Project (GTEx), which includes 515 lung samples and 670 blood samples. While we

sought colocalization with GOLD-defined COPD, we expect that other respiratory- or smoking-related genetic associations would benefit from the use of this resource. One potential weakness is that our RNASeq was performed using whole lung tissue and whole blood samples, which contain a variety of cell types. Therefore, some of the changes in transcriptional splicing detected may actually be reflecting differences in inter-individual cell proportions. Another limitation is the use of Moloc, which attempts colocalization with the most significant signal in the region, and may not be optimal in the setting of multiple QTL or GWAS signals in the region. Additional work characterizing splicing using single-cell short or long read RNASeq is required.

In conclusion, we discovered that multiple COPD GWAS associations colocalize with sQTLs, and identify or replicate several candidate genes as COPD targets for follow-up.



## **Funding/Acknowledgements**

This work was funded by K01HL157613, R01HL157879, P01HL114501, X01HL139404, R01HL124233, R01HL126596, R01HL153248, R01HL149861, R01 HL111527HL135142, and NIGMS R35 GM140844.

Molecular data for the Trans-Omics in Precision Medicine (TOPMed) program was supported by the National Heart, Lung and Blood Institute (NHLBI). Whole Genome Sequencing and RNASeq for "NHLBI TOPMed: The Lung Tissue Research Consortium (phs001662)" was performed at Northwest Genome Center (NWGC, HHSN268201600032I, RNASeq) and Broad Genomics (HHSN268201600034I, WGS) Core support including centralized genomic read mapping and genotype calling, along with variant quality metrics and filtering were provided by the TOPMed Informatics Research Center (3R01HL-117626-02S1; contract HHSN268201800002I). Core support including phenotype harmonization, data management, sample-identity QC, and general program coordination were provided by the TOPMed Data Coordinating Center (R01HL-120393; U01HL-120393; contract HHSN268201800001I). We gratefully acknowledge the studies and participants who provided biological samples and data for TOPMed..

The COPDGene study (NCT00608764) is supported by grants from the NHLBI (U01HL089897 and U01HL089856), by NIH contract 75N92023D00011, and by the COPD Foundation through contributions made to an Industry Advisory Committee that has included AstraZeneca, Bayer Pharmaceuticals, Boehringer-Ingelheim, Genentech, GlaxoSmithKline, Novartis, Pfizer and Sunovion.

This study utilized biological specimens and data provided by the Lung Tissue Research Consortium (LTRC) supported by the National Heart, Lung, and Blood Institute (NHLBI).

## **COPDGene® Investigators – Core Units**

*Administrative Center:* James D. Crapo, MD (PI); Edwin K. Silverman, MD, PhD (PI); Barry J. Make, MD; Elizabeth A. Regan, MD, PhD

*Genetic Analysis Center:* Terri H. Beaty, PhD; Peter J. Castaldi, MD, MSc; Michael H. Cho, MD, MPH; Dawn L. DeMeo, MD, MPH; Adel El Boueiz, MD, MMSc; Marilyn G. Foreman, MD, MS; Auyon Ghosh, MD; Lystra P. Hayden, MD, MMSc; Craig P. Hersh, MD, MPH; Jacqueline Hetmanski, MS; Brian D. Hobbs, MD, MMSc; John E. Hokanson, MPH, PhD; Wonji Kim, PhD; Nan Laird, PhD; Christoph Lange, PhD; Sharon M. Lutz, PhD; Merry-Lynn McDonald, PhD; Dmitry Prokopenko, PhD; Matthew Moll, MD, MPH; Jarrett Morrow, PhD; Dandi Qiao, PhD; Elizabeth A. Regan, MD, PhD; Aabida Saferali, PhD; Phuwant Sakornsakolpat, MD; Edwin K. Silverman, MD, PhD; Emily S. Wan, MD; Jeong Yun, MD, MPH

*Imaging Center:* Juan Pablo Centeno; Jean-Paul Charbonnier, PhD; Harvey O. Coxson, PhD; Craig J. Galban, PhD; MeiLan K. Han, MD, MS; Eric A. Hoffman, Stephen Humphries, PhD; Francine L. Jacobson, MD, MPH; Philip F. Judy, PhD; Ella A. Kazerooni, MD; Alex Kluber; David A. Lynch, MB; Pietro Nardelli, PhD; John D. Newell, Jr., MD; Aleena Notary; Andrea Oh, MD; Elizabeth A. Regan, MD, PhD; James C. Ross, PhD; Raul San Jose Estepar, PhD; Joyce Schroeder, MD; Jered Sieren; Berend C. Stoel, PhD; Juerg Tschirren, PhD; Edwin Van Beek, MD, PhD; Bram van Ginneken, PhD; Eva van Rikxoort, PhD; Gonzalo Vegas SanchezFerrero, PhD; Lucas Veitel; George R. Washko, MD; Carla G. Wilson, MS;

*PFT QA Center, Salt Lake City, UT:* Robert Jensen, PhD

*Data Coordinating Center and Biostatistics, National Jewish Health, Denver, CO:* Douglas Everett, PhD; Jim Crooks, PhD; Katherine Pratte, PhD; Matt Strand, PhD; Carla G. Wilson, MS  
*Epidemiology Core, University of Colorado Anschutz Medical Campus, Aurora, CO:* John E. Hokanson, MPH, PhD; Erin Austin, PhD; Gregory Kinney, MPH, PhD; Sharon M. Lutz, PhD; Kendra A. Young, PhD  
Version Date: March 26, 2021

*Mortality Adjudication Core:* Surya P. Bhatt, MD; Jessica Bon, MD; Alejandro A. Diaz, MD, MPH; MeiLan K. Han, MD, MS; Barry Make, MD; Susan Murray, ScD; Elizabeth Regan, MD; Xavier Soler, MD; Carla G. Wilson, MS

*Biomarker Core:* Russell P. Bowler, MD, PhD; Katerina Kechris, PhD; Farnoush BanaeiKashani, PhD

## **COPDGene® Investigators – Clinical Centers**

*Ann Arbor VA:* Jeffrey L. Curtis, MD; Perry G. Pernicano, MD

*Baylor College of Medicine, Houston, TX:* Nicola Hanania, MD, MS; Mustafa Atik, MD; Aladin Boriek, PhD; Kalpatha Guntupalli, MD; Elizabeth Guy, MD; Amit Parulekar, MD;

*Brigham and Women's Hospital, Boston, MA:* Dawn L. DeMeo, MD, MPH; Craig Hersh, MD, MPH; Francine L. Jacobson, MD, MPH; George Washko, MD

*Columbia University, New York, NY:* R. Graham Barr, MD, DrPH; John Austin, MD; Belinda D'Souza, MD; Byron Thomashow, MD

*Duke University Medical Center, Durham, NC:* Neil MacIntyre, Jr., MD; H. Page McAdams, MD; Lacey Washington, MD

*HealthPartners Research Institute, Minneapolis, MN:* Charlene McEvoy, MD, MPH; Joseph Tashjian, MD

*Johns Hopkins University, Baltimore, MD:* Robert Wise, MD; Robert Brown, MD; Nadia N. Hansel, MD, MPH; Karen Horton, MD; Allison Lambert, MD, MHS; Nirupama Putcha, MD, MHS

*Lundquist Institute for Biomedical Innovation at Harbor UCLA Medical Center, Torrance, CA:* Richard Casaburi, PhD, MD; Alessandra Adami, PhD; Matthew Budoff, MD; Hans Fischer, MD; Janos Porszasz, MD, PhD; Harry Rossiter, PhD; William Stringer, MD

*Michael E. DeBakey VAMC, Houston, TX:* Amir Sharafkhaneh, MD, PhD; Charlie Lan, DO

*Minneapolis VA:* Christine Wendt, MD; Brian Bell, MD; Ken M. Kunisaki, MD, MS

*Morehouse School of Medicine, Atlanta, GA:* Eric L. Flenaugh, MD; Hirut Gebrekristos, PhD; Mario Ponce, MD; Silanath Terpenning, MD; Gloria Westney, MD, MS

*National Jewish Health, Denver, CO:* Russell Bowler, MD, PhD; David A. Lynch, MB

*Reliant Medical Group, Worcester, MA:* Richard Rosiello, MD; David Pace, MD

*Temple University, Philadelphia, PA:* Gerard Criner, MD; David Ciccolella, MD; Francis Cordova, MD; Chandra Dass, MD; Gilbert D'Alonzo, DO; Parag Desai, MD; Michael Jacobs, PharmD; Steven Kelsen, MD, PhD; Victor Kim, MD; A. James Mamary, MD; Nathaniel Version Date: March 26, 2021 Marchetti, DO; Aditi Satti, MD; Kartik Shenoy, MD; Robert M. Steiner, MD; Alex Swift, MD; Irene Swift, MD; Maria Elena Vega-Sanchez, MD

*University of Alabama, Birmingham, AL:* Mark Dransfield, MD; William Bailey, MD; Surya P. Bhatt, MD; Anand Iyer, MD; Hrudaya Nath, MD; J. Michael Wells, MD

*University of California, San Diego, CA:* Douglas Conrad, MD; Xavier Soler, MD, PhD; Andrew Yen, MD

*University of Iowa, Iowa City, IA:* Alejandro P. Comellas, MD; Karin F. Hoth, PhD; John Newell, Jr., MD; Brad Thompson, MD

*University of Michigan, Ann Arbor, MI:* MeiLan K. Han, MD MS; Ella Kazerooni, MD MS; Wassim Labaki, MD MS; Craig Galban, PhD; Dharshan Vummidi, MD

*University of Minnesota, Minneapolis, MN:* Joanne Billings, MD; Abbie Begnaud, MD; Tadashi Allen, MD

*University of Pittsburgh, Pittsburgh, PA:* Frank Sciruba, MD; Jessica Bon, MD; Divay Chandra, MD, MSc; Joel Weissfeld, MD, MPH

*University of Texas Health, San Antonio, San Antonio, TX:* Antonio Anzueto, MD; Sandra Adams, MD; Diego Maselli-Caceres, MD; Mario E. Ruiz, MD; Harjinder Singh

## **Data and Code Availability**

LTRC genotyping data are available on dbGaP with accession number phs001662.v1.p1

LTRC RNA-seq data are available through TOPMed, <https://topmed.nhlbi.nih.gov>. COPDGene

data are available on dbGaP with accession numbers phs000179 and phs000765.

## Tables

**Table 1: Clinical characteristics of LTRC and COPDGene study individuals included in the analysis.**

	<b>LTRC (n=1241)</b>	<b>COPDGene (n=3734)</b>
Gender, male (%)	52.4	51.1
Age, mean (SD)	63.3 (10.6)	59.9 (8.7)
Race, <i>n</i> (%)		
White	White 1118 (90.1)	2702 (72.4)
	Asian 4 (0.3)	--
	Black 81 (6.5)	1032 (27.6)
	Hispanic 25 (2.0)	--
	Other 13 (1.0)	--
Current Smokers, <i>n</i> (%)*	73 (5.9)	1766 (47.3)
Pack-Years Smoked, mean (SD)	31.8 (+/-33.2)	42.7 (+/-24.0)

\*Smoking data is missing for a subset of LTRC subjects

**Table 2: Summary of expressionQTLs and spliceQTLs tested**

	<b>COPDGene</b>			<b>LTRC</b>		
	<b>Genes</b>	<b>Splice Sites</b>		<b>Genes</b>	<b>Splice Sites</b>	
		<b>introns</b>	<b>clusters</b>		<b>introns</b>	<b>clusters</b>
<b>Before filtering</b>	60,232	237,155	58,318	58,962	306,475	70,094
<b>After filtering</b>	15,507	160,655	35,358	16,266	223,154	48,095
<b>Genes tested</b>	15,507	12096		16,266	18,777	
<b>SNPs tested</b>	11,869,333			8,792,206		
<b>Significant QTL<sup>1</sup></b>	15,279	60,291	18,294	11,615	58,258	18,688

<sup>1</sup>The number of genes or splice sites significantly associated with at least one SNP with FDR<0.05.

**Table 3: Annotations of Leafcutter Splice Sites Identified in COPDGene and LTRC**

	<b>Frequency in LTRC</b>	<b>Percent in LTRC</b>	<b>Frequency in COPDGene</b>	<b>Percent in COPDGene</b>
<b>Annotated<sup>1</sup></b>	113562	50.9	81111	50.5
<b>Cryptic 5'</b>	30166	13.5	21232	13.2
<b>Cryptic 3'</b>	32258	14.5	24047	15.0
<b>Cryptic unanchored</b>	8504	3.8	5788	3.6
<b>Novel annotated pair</b>	17991	8.1	13293	8.3
<b>Unknown strand</b>	20626	9.2	15166	9.4

<sup>1</sup>Annotated = both 5' and 3' splice sites have been previously annotated; Cryptic fiveprime = the 5' splice site is not annotated but the 3' splice site is annotated; Cryptic threeprime = the 3' splice site is not annotated but the 5' splice site is annotated; Cryptic unanchored = neither splice site has been previously annotated; Novel annotated pair = both 5' and 3' splice sites have been individually annotated but the combination have not been annotated as a junction; Unknown strand = it is not possible to determine the directionality of the splice sites based on the RNASeq read.

**Table 4: Annotation of QTL variants in relation to the gene body**

Annotation	COPDGene		LTRC	
	eQTLs (%)	sQTLs (%)	eQTLs (%)	sQTLs (%)
<b>Upstream gene variant</b>	32.1	34.7	31.8	29.4
<b>Intron variant</b>	24.4	20.9	25.2	25.8
<b>Downstream gene variant</b>	14.5	10.8	14.9	15.8
<b>Intergenic region</b>	11.9	7.0	10.6	11.4
<b>3 prime UTR variant</b>	5.0	6.8	5.7	3.3
<b>5 prime UTR variant</b>	3.1	4.4	3.6	2.2
<b>Missense variant</b>	2.1	3.5	2.2	3.3
<b>Synonymous variant</b>	1.9	2.8	1.8	3.2
<b>other</b>	4.9	3.8	2.8	4.2



**Table 5: Summary of Colocalization Analysis**

Best Colocalized SNP <sup>1</sup>	PPA <sup>2</sup>	Lead QTL					GWAS	
		Gene <sup>2</sup>	QTL Type	Splice site	p-value	Effect <sup>3</sup>	p-value	Effect <sup>3</sup>
4:144567946:A:G	0.973	<i>HHIP</i>	LTRC_sQTL	4:144734889-144737129	0.00610	0.104	4.09E-59	16.136
4:105897896:G:A	0.999	<i>NPNT</i>	LTRC_sQTL	4:105927428-105931515	8.12E-10	0.114	3.04E-46	14.331
5:148475407:C:T	0.973	<i>FBXO38</i>	LTRC_sQTL	5:148414306-148415928	0.00333	-0.195	2.58E-33	-12.010
15:71329185:G:A	0.992	<i>THSD4</i>	LTRC_eQTL	ENSG00000187720.14	0.154	4.653	1.58E-32	11.852
16:75439564:G:A	0.933	<i>TMEM170A</i>	COPDGene_sQTL	16:75451839-75464232	7.63E-08	0.187	1.26E-20	9.277
6:30814428:G:C	0.987	<i>IER3</i>	COPDGene_sQTL	6:30744196-30744279	0.000119	-0.176	1.41E-20	9.295
4:88948181:T:C	0.832	<i>PKD2</i>	COPDGene_sQTL	4:88019571-88035071	3.76E-08	-0.518	4.23E-18	-8.722
6:32660630:T:C	0.997	<i>HLA-DRB5</i>	COPDGene_sQTL	6:32520345-32555661	6.09E-15	-0.275	5.56E-18	-8.661
5:157505976:A:T	0.968	<i>ADAM19</i>	LTRC_eQTL	ENSG00000135074.15	8.62E-10	2.468	1.22E-16	-8.324
3:128242335:T:A	0.935	<i>EEFSEC</i>	COPDGene_sQTL	3:128195329-128246836	0.0014	0.032	3.53E-15	7.897
6:29639324:T:C	0.997	<i>HLA-E</i>	COPDGene_sQTL	6:30490515-30491137	4.82E-301	-0.890	4.35E-15	-7.864
6:27420975:T:C	0.976	<i>ZKSCAN4</i>	COPDGene_sQTL	6:28249834-28251867	5.35E-20	0.308	3.58E-14	-7.573
6:28651576:A:G	0.996	<i>GABBR1</i>	COPDGene_eQTL	ENSG00000204681.11	3.96E-17	-2.034	3.82E-14	-7.556
6:26409662:G:C	0.905	<i>BTN2A1</i>	LTRC_sQTL	6:26459828-26463244	1.79E-10	-0.486	1.03E-13	7.449
6:32775967:G:A	0.982	<i>HLA-DRB5</i>	COPDGene_sQTL	6:32481801-32525584	8.02E-09	-0.222	3.76E-12	6.955
2:238965524:G:A	0.941	<i>TWIST2</i>	LTRC_eQTL	ENSG00000233608.4	0.0483	0.269	2.17E-11	-6.699
3:25496178:G:A	0.990	<i>RARB</i>	LTRC_eQTL	ENSG00000077092.19	2.60E-06	0.925	5.84E-11	-6.570
2:9145396:G:A	0.956	<i>LINC00299</i>	COPDGene_sQTL	2:8299793-8312726	0.0479	-0.115	2.41E-10	6.343
1:16979534:C:A	0.990	<i>CROCC</i>	COPDGene_sQTL	1:16922798-16924325	0.000528	-0.121	6.55E-10	6.192
7:100032719:C:T	0.994	<i>ZSCAN21</i>	COPDGene_sQTL	7:100049841-100051478	6.28E-05	-0.153	7.26E-10	-6.175
19:45790878:G:A	0.998	<i>DMWD</i>	LTRC_APAQTL	ENST00000597053.1	0.00118	-0.044	1.67E-09	-6.009
1:39582337:G:A	0.933	<i>PPIEL</i>	COPDGene_sQTL	1:39548951-39554349	0.0176	-0.128	1.98E-09	6.009
12:95843792:T:C	0.972	<i>NTN4</i>	LTRC_sQTL	12:95713338-95717545	6.56E-09	-0.400	2.64E-09	-5.935
4:74748514:C:T	0.951	<i>BTC</i>	LTRC_sQTL	4:74748149-74750573	0.00187	-0.238	3.45E-09	-5.903
1:111195294:T:C	0.850	<i>DENND2D</i>	COPDGene_sQTL	1:111194726-111195668	0.00843	-0.556	3.59E-09	-5.892
14:92649065:G:C	0.963	<i>RIN3</i>	LTRC_APAQTL	ENST00000553992.1	0.00115	-0.025	6.69E-09	5.795
1:239689643:G:C	0.968	<i>CHRM3-AS2</i>	COPDGene_APAQTL	ENST00000593855	2.77E-48	-0.279	9.61E-09	5.755
11:13145018:T:C	0.941	<i>RASSF10</i>	LTRC_eQTL	ENSG00000189431.7	4.27E-09	0.250	1.18E-08	5.717
5:151215512:A:G	0.994	<i>GM2A</i>	LTRC_APAQTL	ENST00000523004.1	9.43E-100	0.011	1.40E-08	-5.695
7:2830820:T:G	0.873	<i>GNA12</i>	LTRC_sQTL	7:2733501-2762829	0.00185	0.156	1.74E-08	5.648
17:38730575:G:A	0.990	<i>CISD3</i>	LTRC_eQTL	ENSG00000277972.1	8.70E-11	-2.872	1.90E-08	5.620

3:29430921:G:C	0.985	<i>RBMS3</i>	LTRC_eQTL	ENSG00000144642.21	1.02E-11	-2.128	2.04E-08	5.636
15:49578340:A:G	0.943	<i>FAM227B</i>	LTRC_sQTL	15:49589745-49606156	0.0146	-0.151	2.82E-08	5.564
16:58063696:G:C	0.890	<i>MMP15</i>	LTRC_sQTL	16:58040698-58041617	0.0122	0.274	4.26E-08	5.500
10:80458350:G:C	0.995	<i>TSPAN14</i>	COPDGene_sQTL	10:80459507-80463088	3.64E-07	0.132	4.30E-08	-5.465
1:45543641:G:C	0.959	<i>TESK2</i>	COPDGene_APAQTL	ENST00000486676	0.00967	-0.032	4.67E-08	-5.485
2:42206107:C:T	0.980	<i>COX7A2L</i>	COPDGene_APAQTL	ENST00000463055	NA	NA	4.85E-08	-5.446
17:30129740:C:T	0.865	<i>NSRP1</i>	COPDGene_sQTL	17:30118173-30156218	0.000150	0.116	4.86E-08	5.480

<sup>1</sup>SNP = chromosome, position, reference, and effect allele, where position is build 38.

<sup>2</sup>PPA = posterior probability of association from moloc software. For some loci, there were multiple colocalizations between QTLs and GWAS data, the results for the association with the highest PPA is reported here

<sup>3</sup>The direction of the effect size is based on the second allele listed in the variant ID

**Figure 1**

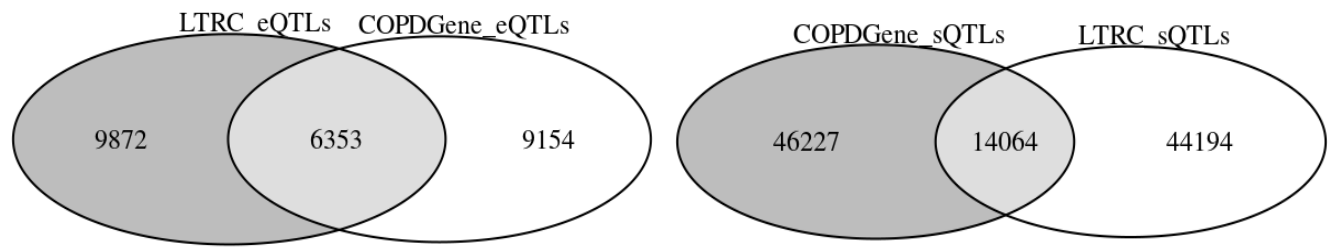


**Figure 1:** Overlap between LTRC lung and COPDGene blood eQTLs and sQTLs that were significant at  $FDR < 0.05$

Figure 2:

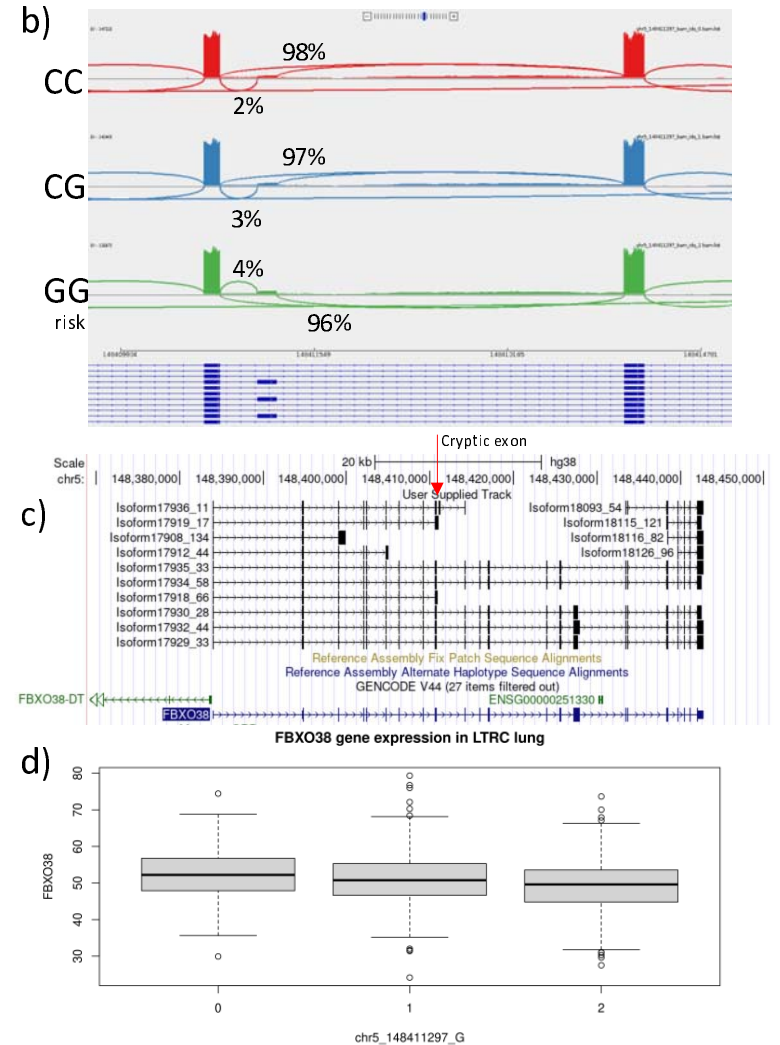
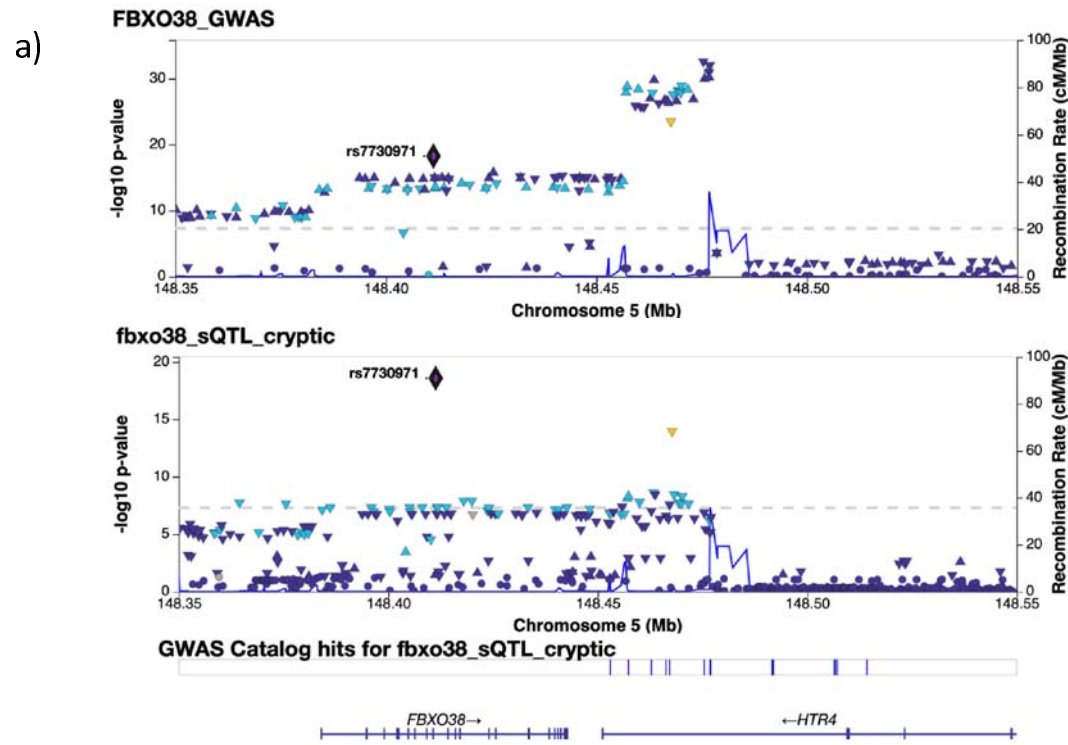


**Figure 2: Replication of *FBXO38* sQTL findings in lung tissue.**

a) Locus association plot for COPD GWAS and *FBXO38* sQTL. The lead SNP associated with *FBXO38* splicing, rs7730971, is highlighted in purple and used as the LD reference. b) IGV sashimi plot showing the region spanning chr5:148409934-148414781 for 191 subjects from each genotype of rs7730971. c) Long read sequencing data showing all *FBXO38* isoforms representing at least 1% of total *FBXO38* expression. The cryptic exon is identified with a red arrow. D) Boxplot of total gene expression values for *FBXO38*.

Figure 3:

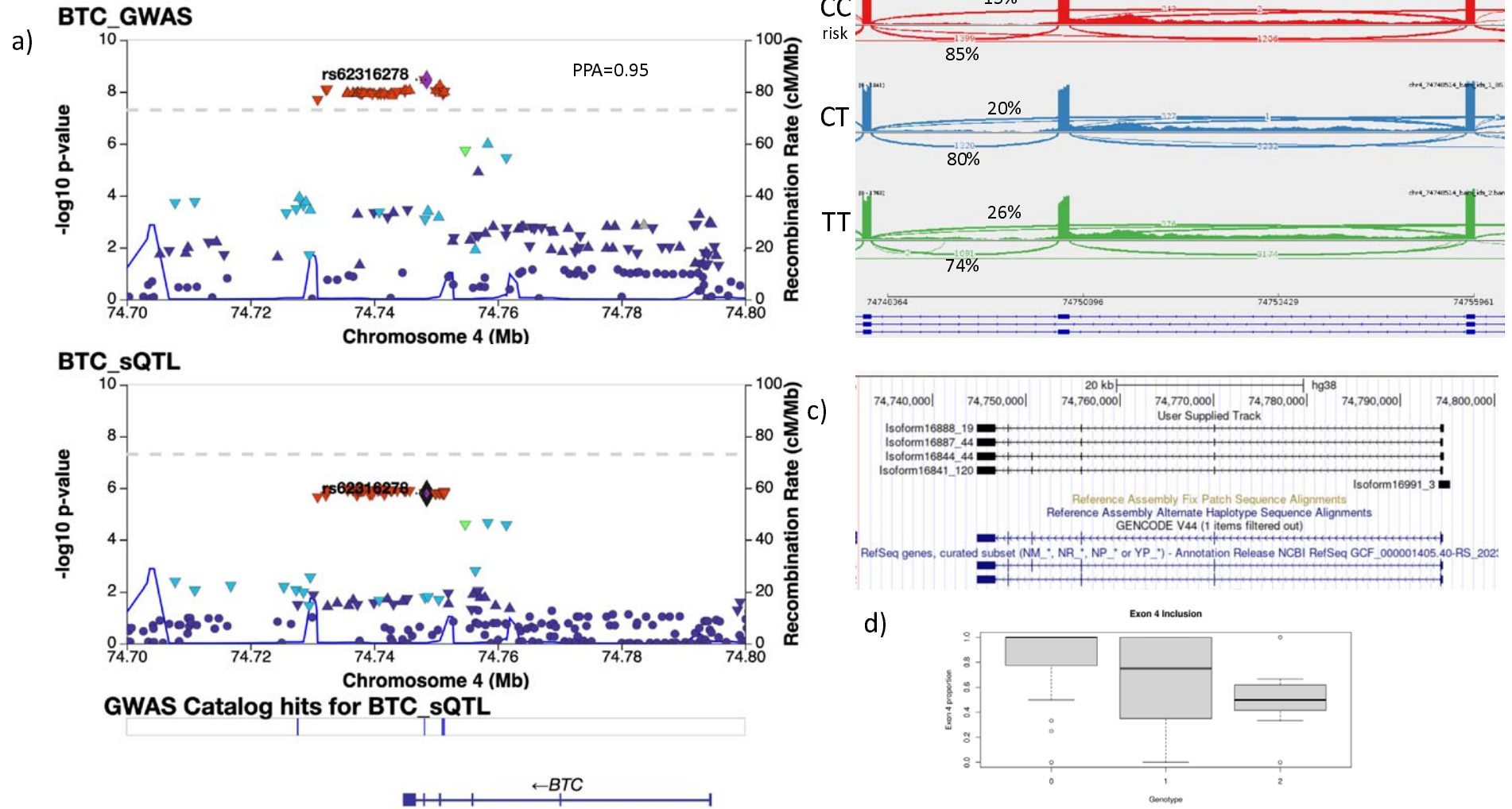


**Figure 3: sQTLs for *BTC* colocalize with GWAS data for COPD.** a) Locus association plot for COPD GWAS and *BTC* sQTL. The lead colocalized SNP, rs62316278, is highlighted in purple and used as the LD reference. b) IGV sashimi plot showing the region spanning chr4:74748364-74755961 for 86 subjects from each genotype of rs62316278. c) Long read sequencing data showing all *BTC* isoforms representing at least 10% of total *BTC* expression. d) Proportion of *BTC* expression of isoforms containing exon 4 by copies of rs62316278-T.

## **References**

1. Sakornsakolpat P, Prokopenko D, Lamontagne M, Reeve NF, Guyatt AL, Jackson VE, et al. Genetic landscape of chronic obstructive pulmonary disease identifies heterogeneous cell-type and phenotype associations. *Nat Genet.* 2019;51(3):494-505. Epub 2019/02/26. doi: 10.1038/s41588-018-0342-2. PubMed PMID: 30804561; PubMed Central PMCID: PMC6546635.
2. Cohen BH, Ball WC, Jr., Brashears S, Diamond EL, Kreiss P, Levy DA, et al. Risk factors in chronic obstructive pulmonary disease (COPD). *Am J Epidemiol.* 1977;105(3):223-32. Epub 1977/03/01. doi: 10.1093/oxfordjournals.aje.a112378. PubMed PMID: 300564.
3. Kueppers F, Miller RD, Gordon H, Hepper NG, Offord K. Familial prevalence of chronic obstructive pulmonary disease in a matched pair study. *Am J Med.* 1977;63(3):336-42. Epub 1977/09/01. doi: 10.1016/0002-9343(77)90270-4. PubMed PMID: 302643.
4. McCloskey SC, Patel BD, Hinchliffe SJ, Reid ED, Wareham NJ, Lomas DA. Siblings of patients with severe chronic obstructive pulmonary disease have a significant risk of airflow obstruction. *Am J Respir Crit Care Med.* 2001;164(8 Pt 1):1419-24. Epub 2001/11/13. doi: 10.1164/ajrccm.164.8.2105002. PubMed PMID: 11704589.
5. Silverman EK, Chapman HA, Drazen JM, Weiss ST, Rosner B, Campbell EJ, et al. Genetic epidemiology of severe, early-onset chronic obstructive pulmonary disease. Risk to relatives for airflow obstruction and chronic bronchitis. *Am J Respir Crit Care Med.* 1998;157(6 Pt 1):1770-8. Epub 1998/06/25. doi: 10.1164/ajrccm.157.6.9706014. PubMed PMID: 9620904.
6. Hobbs BD, de Jong K, Lamontagne M, Bosse Y, Shrine N, Artigas MS, et al. Genetic loci associated with chronic obstructive pulmonary disease overlap with loci for lung function and pulmonary fibrosis. *Nat Genet.* 2017;49(3):426-32. Epub 2017/02/07. doi: 10.1038/ng.3752. PubMed PMID: 28166215; PubMed Central PMCID: PMC5381275.
7. Shrine N, Guyatt AL, Erzurumluoglu AM, Jackson VE, Hobbs BD, Melbourne CA, et al. New genetic signals for lung function highlight pathways and chronic obstructive pulmonary disease associations across multiple ancestries. *Nat Genet.* 2019;51(3):481-93. Epub 2019/02/26. doi: 10.1038/s41588-018-0321-7. PubMed PMID: 30804560; PubMed Central PMCID: PMC6397078.
8. Shrine N, Izquierdo AG, Chen J, Packer R, Hall RJ, Guyatt AL, et al. Multi-ancestry genome-wide association analyses improve resolution of genes and pathways influencing lung function and chronic obstructive pulmonary disease risk. *Nat Genet.* 2023;55(3):410-22. Epub 2023/03/15. doi: 10.1038/s41588-023-01314-0. PubMed PMID: 36914875; PubMed Central PMCID: PMC10011137 research projects outside of the submitted work. I.P.H. has funded research collaborations with GSK, Boehringer Ingelheim and Orion. M.H.C. has received grant funding from GSK and Bayer, and speaking or consulting fees from AstraZeneca, Illumina and Genentech. B.D.H. has received grant funding from Bayer and speaking or consulting fees from AstraZeneca. I.S. has funded research collaborations with GSK, Boehringer Ingelheim and Orion outside of the submitted work. R.J.P., M.D.T., C.J. and L.V.W. have a funded research collaboration with Orion for collaborative research projects outside of the submitted work. The other authors declare no competing interests.
9. Gamazon ER, Segre AV, van de Bunt M, Wen X, Xi HS, Hormozdiari F, et al. Using an atlas of gene regulation across 44 human tissues to inform complex disease- and trait-associated variation. *Nat Genet.* 2018;50(7):956-67. Epub 2018/06/30. doi: 10.1038/s41588-018-0154-4. PubMed PMID: 29955180; PubMed Central PMCID: PMC6248311.

10. Saferali A, Yun JH, Parker MM, Sakornsakolpat P, Chase RP, Lamb A, et al. Analysis of genetically driven alternative splicing identifies FBXO38 as a novel COPD susceptibility gene. *PLoS Genet.* 2019;15(7):e1008229. Epub 2019/07/04. doi: 10.1371/journal.pgen.1008229. PubMed PMID: 31269066; PubMed Central PMCID: PMC6634423.
11. Barbeira AN, Dickinson SP, Bonazzola R, Zheng J, Wheeler HE, Torres JM, et al. Exploring the phenotypic consequences of tissue specific gene expression variation inferred from GWAS summary statistics. *Nat Commun.* 2018;9(1):1825. Epub 2018/05/10. doi: 10.1038/s41467-018-03621-1. PubMed PMID: 29739930; PubMed Central PMCID: PMC65940825.
12. Regan EA, Hokanson JE, Murphy JR, Make B, Lynch DA, Beaty TH, et al. Genetic epidemiology of COPD (COPDGene) study design. *COPD.* 2010;7(1):32-43. Epub 2010/03/11. doi: 10.3109/15412550903499522. PubMed PMID: 20214461; PubMed Central PMCID: PMC62924193.
13. Ghosh AJ, Hobbs BD, Yun JH, Saferali A, Moll M, Xu Z, et al. Lung tissue shows divergent gene expression between chronic obstructive pulmonary disease and idiopathic pulmonary fibrosis. *Respir Res.* 2022;23(1):97. Epub 2022/04/23. doi: 10.1186/s12931-022-02013-w. PubMed PMID: 35449067; PubMed Central PMCID: PMC9026726.
14. Parker MM, Chase RP, Lamb A, Reyes A, Saferali A, Yun JH, et al. RNA sequencing identifies novel non-coding RNA and exon-specific effects associated with cigarette smoking. *BMC Medical Genomics.* 2017;10(1):58-.
15. Patro R, Duggal G, Love MI, Irizarry RA, Kingsford C. Salmon provides fast and bias-aware quantification of transcript expression. *Nat Methods.* 2017;14(4):417-9. Epub 2017/03/07. doi: 10.1038/nmeth.4197. PubMed PMID: 28263959; PubMed Central PMCID: PMC65600148.
16. Sonesson C, Love MI, Robinson MD. Differential analyses for RNA-seq: transcript-level estimates improve gene-level inferences. *F1000Res.* 2015;4:1521. Epub 2016/03/01. doi: 10.12688/f1000research.7563.2. PubMed PMID: 26925227; PubMed Central PMCID: PMC64712774.
17. Li YI, Knowles DA, Humphrey J, Barbeira AN, Dickinson SP, Im HK, et al. Annotation-free quantification of RNA splicing using LeafCutter. *Nat Genet.* 2018;50(1):151-8. Epub 2017/12/13. doi: 10.1038/s41588-017-0004-9. PubMed PMID: 29229983; PubMed Central PMCID: PMC65742080.
18. Risso D, Ngai J, Speed TP, Dudoit S. Normalization of RNA-seq data using factor analysis of control genes or samples. *Nat Biotechnol.* 2014;32(9):896-902. Epub 2014/08/26. doi: 10.1038/nbt.2931. PubMed PMID: 25150836; PubMed Central PMCID: PMC64404308.
19. Taylor-Weiner A, Aguet F, Haradhvala NJ, Gosai S, Anand S, Kim J, et al. Scaling computational genomics to millions of individuals with GPUs. *Genome Biol.* 2019;20(1):228. Epub 2019/11/05. doi: 10.1186/s13059-019-1836-7. PubMed PMID: 31675989; PubMed Central PMCID: PMC6823959 GG have filed a patent application related to the methods described in this work. GG receives research funds from IBM and Pharmacyclics. GG is an inventor on multiple bioinformatics-related patent applications. EMV is a consultant for Tango Therapeutics, Genome Medical, Invitae, Foresite Capital, and Illumina. EMV received research support from Novartis and BMS, as well as travel support from Roche/Genentech. EMV is an equity holder of Syapse, Tango Therapeutics, and Genome Medical. EMV holds stock in Microsoft. Broad permits non-profit institutions and government agencies to operate under Broad patents to

conduct internal research, including sponsored research to the extent such research does not include the production or manufacture of products for sale or offer for sale or performance of commercial services for a fee.

20. Cho MH, Castaldi PJ, Wan ES, Siedlinski M, Hersh CP, Demeo DL, et al. A genome-wide association study of COPD identifies a susceptibility locus on chromosome 19q13. *Hum Mol Genet.* 2012;21(4):947-57. Epub 2011/11/15. doi: 10.1093/hmg/ddr524. PubMed PMID: 22080838; PubMed Central PMCID: PMCPMC3298111.
21. Wang K, Li M, Hakonarson H. ANNOVAR: functional annotation of genetic variants from high-throughput sequencing data. *Nucleic Acids Res.* 2010;38(16):e164. Epub 2010/07/06. doi: 10.1093/nar/gkq603. PubMed PMID: 20601685; PubMed Central PMCID: PMCPMC2938201.
22. Giambartolomei C, Zhenli Liu J, Zhang W, Hauberg M, Shi H, Boocock J, et al. A Bayesian framework for multiple trait colocalization from summary association statistics. *Bioinformatics.* 2018;34(15):2538-45. Epub 2018/03/27. doi: 10.1093/bioinformatics/bty147. PubMed PMID: 29579179; PubMed Central PMCID: PMCPMC6061859.
23. Zou Y, Carbonetto P, Xie D, Wang G, Stephens M. Fast and flexible joint fine-mapping of multiple traits via the Sum of Single Effects model. *bioRxiv.* 2023. Epub 2023/07/10. doi: 10.1101/2023.04.14.536893. PubMed PMID: 37425935; PubMed Central PMCID: PMCPMC10327118.
24. Li YI, Knowles DA, Humphrey J, Barbeira AN, Dickinson SP, Im HK, et al. Annotation-free quantification of RNA splicing using LeafCutter. *Nature Genetics.* 2018;50(1):151-158.
25. Saferali A, Kim W, Xu Z, Chase RP, Cho MH, Laederach A, et al. Colocalization analysis of 3' UTR alternative polyadenylation quantitative trait loci reveals novel mechanisms underlying associations with lung function. *Hum Mol Genet.* 2024. Epub 2024/04/04. doi: 10.1093/hmg/ddae055. PubMed PMID: 38569558.
26. Saferali A, Xu Z, Sheynkman GM, Hersh CP, Cho MH, Silverman EK, et al. Characterization of a COPD-Associated NPNT Functional Splicing Genetic Variant in Human Lung Tissue via Long-Read Sequencing. *medRxiv.* 2020. Epub 2020/11/12. doi: 10.1101/2020.10.20.20203927. PubMed PMID: 33173926; PubMed Central PMCID: PMCPMC7654922.
27. Morrow JD, Zhou X, Lao T, Jiang Z, Demeo DL, Cho M, et al. Functional interactors of three genome-wide association study genes are differentially expressed in severe chronic obstructive pulmonary disease lung tissue. *Scientific reports.* 2017;7(1):44232-.
28. Hormozdiari F, van de Bunt M, Segre AV, Li X, Joo JWW, Bilow M, et al. Colocalization of GWAS and eQTL Signals Detects Target Genes. *American Journal of Human Genetics.* 2016;99(6):1245-1260.
29. Jaganathan K, Kyriazopoulou Panagiotopoulou S, McRae JF, Darbandi SF, Knowles D, Li YI, et al. Predicting Splicing from Primary Sequence with Deep Learning. *Cell.* 2019;176(3):535-48 e24. Epub 2019/01/22. doi: 10.1016/j.cell.2018.12.015. PubMed PMID: 30661751.
30. Zhang Z, Xin D, Wang P, Zhou L, Hu L, Kong X, et al. Noisy splicing, more than expression regulation, explains why some exons are subject to nonsense-mediated mRNA decay. *BMC Biol.* 2009;7:23. Epub 2009/05/16. doi: 10.1186/1741-7007-7-23. PubMed PMID: 19442261; PubMed Central PMCID: PMCPMC2697156.



31. Kipreos ET, Pagano M. The F-box protein family. *Genome Biol.* 2000;1(5):REVIEWS3002. Epub 2001/02/24. doi: 10.1186/gb-2000-1-5-reviews3002. PubMed PMID: 11178263; PubMed Central PMCID: PMCPMC138887.
32. Smaldone S, Laub F, Else C, Dragomir C, Ramirez F. Identification of MoKA, a novel F-box protein that modulates Kruppel-like transcription factor 7 activity. *Mol Cell Biol.* 2004;24(3):1058-69. Epub 2004/01/20. doi: 10.1128/MCB.24.3.1058-1069.2004. PubMed PMID: 14729953; PubMed Central PMCID: PMCPMC321422.
33. Smaldone S, Ramirez F. Multiple pathways regulate intracellular shuttling of MoKA, a co-activator of transcription factor KLF7. *Nucleic Acids Res.* 2006;34(18):5060-8. Epub 2006/09/23. doi: 10.1093/nar/gkl659. PubMed PMID: 16990251; PubMed Central PMCID: PMCPMC1636432.
34. Dunbar AJ, Goddard C. Structure-function and biological role of betacellulin. *Int J Biochem Cell Biol.* 2000;32(8):805-15. Epub 2000/08/15. doi: 10.1016/s1357-2725(00)00028-5. PubMed PMID: 10940639.
35. Serban KA, Pratte KA, Strange C, Sandhaus RA, Turner AM, Beiko T, et al. Unique and shared systemic biomarkers for emphysema in Alpha-1 Antitrypsin deficiency and chronic obstructive pulmonary disease. *EBioMedicine.* 2022;84:104262. Epub 2022/09/27. doi: 10.1016/j.ebiom.2022.104262. PubMed PMID: 36155958; PubMed Central PMCID: PMCPMC9507992.
36. Chen H, Song Z, Qian M, Bai C, Wang X. Selection of disease-specific biomarkers by integrating inflammatory mediators with clinical informatics in AECOPD patients: a preliminary study. *J Cell Mol Med.* 2012;16(6):1286-97. Epub 2011/09/03. doi: 10.1111/j.1582-4934.2011.01416.x. PubMed PMID: 21883889; PubMed Central PMCID: PMCPMC3823081.